Journal of Applied Electrochemistry (2026) 56:146
https://doi.org/10.1007/s10800-026-02511-5

RESEARCH ARTICLE

Bismuth-film-coated poly(L-arginine) electrode for zinc detection in Phuket pineapple soils

Anisah Dueraning[1] · Suparat Cotchim[2] · Supaporn Dawan[1] · Warakorn Limbut[2] · Songyos Pramjit[3]

Received: 4 January 2026 / Accepted: 25 April 2026

Abstract

This research reported a glassy carbon electrode modified with electropolymerized poly(L-arginine) (poly(L-Arg))/GCE for the detection of zinc ions (Zn(II)) by anodic stripping voltammetry (ASV). A bismuth (Bi) film was subsequently formed via in situ plating onto the poly(L-Arg)/GCE, resulting in a Bi/poly(L-Arg)/GCE composite electrode. The fabrication and operational conditions were optimized by adjusting the L-Arg concentration, the number of electropolymerization cycles for poly(L-Arg) modification, the Bi(III) concentration, the pH of the acetate buffer solution, the preconcentration potential, and the preconcentration time. Under optimal conditions, the anodic peak current response exhibited a linear increase within the concentration range of 7.5–400 µg L^{-1} (r = 0.999). The detection limit was determined to be 0.78 µg L^{-1}, while the quantitation limit was found to be 2.6 µg L^{-1}, demonstrating excellent sensitivity and accuracy. This modified electrode was successfully applied to detect Zn(II) in soil samples from Phuket pineapple plantations, with recovery rates ranging from 84.1 to 94.7%. The analytical results were also compared with those obtained from inductively coupled plasma–optical emission spectrometry (ICP-OES), demonstrating that this developed sensor offered good accuracy, precision, and reliability.

Graphical abstract

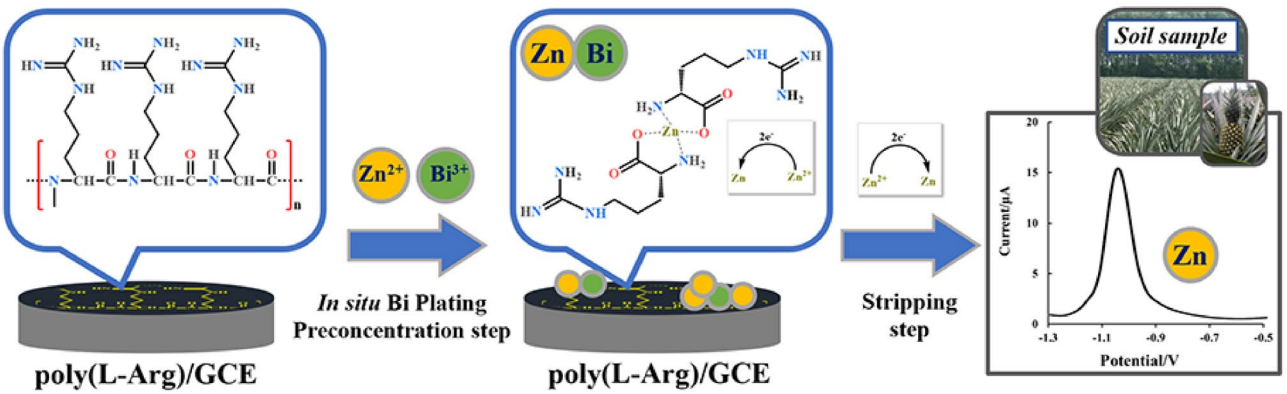

Keywords Zinc · Poly(L-arginine) · Bismuth-film · Anodic stripping voltammetry (ASV) · Phuket pineapple

✉ Anisah Dueraning
anisah.d@pkru.ac.th

[1] Department of Chemistry Education, Faculty of Education, Phuket Rajabhat University, Phuket, Thailand

[2] Division of Health and Applied Sciences, Faculty of Science, Prince of Songkla University, Hat Yai, Songkhla, Thailand

[3] Department of Chemistry, Faculty of Science and Technology, Phuket Rajabhat University, Phuket, Thailand

Published online: 15 June 2026

1 Introduction

Phuket pineapple is an important agricultural product in Thailand [1]. Zinc (Zn) is an essential micronutrient for plant growth and crop quality. It plays a vital role in enzymatic processes, protein and carbohydrate metabolism, and the regulation of auxins, particularly indoleacetic acid (IAA), which is essential for plant development [2]. However, zinc deficiency is a common problem in agricultural soils worldwide [3], including pineapple cultivation in regions such as Hawaii, French Guiana, and Queensland in Australia [2, 4]. This is mainly attributed to the sandy or loamy sand soils in these areas, which have a low nutrient retention capacity. In addition, excessive application of N–P–K fertilizers, particularly phosphate (PO_4^{3-}), can reduce zinc availability through the formation of insoluble zinc phosphate ($Zn_3(PO_4)_2$). Other contributing factors include high soil pH, elevated bicarbonate (HCO_3^-) levels, and nutrient imbalance [5]. The zinc requirement of plants varies depending on the species and their physiological characteristics. In general, the appropriate level of zinc in soil for most crops ranges between 0.5 and 3.0 mg kg^{-1}. For pineapple cultivation, the optimal zinc level in soil is approximately 3 mg kg^{-1} [4]. When the soil zinc concentration falls below 0.5 mg kg^{-1}, it is considered deficiency and may significantly affect plant growth and lead to reduced crop yields [6]. Furthermore, soil zinc content has been reported to correlate with pineapple sweetness and product quality. Therefore, accurate determination of zinc in soil is essential for effective agricultural management and quality control of pineapple production.

Various analytical techniques, including atomic absorption spectrophotometry (AAS) and inductively coupled plasma mass spectrometry (ICP-MS), have been employed for zinc determination. Although these methods provide high sensitivity and accuracy, they require expensive instrumentation, high operating costs, and complicated operations [7, 8]. Electrochemical techniques, particularly anodic stripping voltammetry (ASV), have attracted considerable attention due to their high sensitivity, low detection limits, low reagent consumption, and rapid analysis [7–9]. In the past, the determination of metal ions by ASV predominantly relied on mercury electrodes [7]. However, due to mercury's high toxicity and potential harm to researchers, users, and the environment, there is a growing emphasis on developing analytical methods that align with the principles of green chemistry [10]. As a result, alternative electrode materials, such as metal-based films and carbon-based materials, have been developed to improve environmental compatibility and analytical performance [11–14]. In addition, such materials and surface modifications can offer improved sensitivity, selectivity, and stability, while also supporting miniaturized, portable, and on-site electrochemical analysis [15]. Polymer film-modified electrodes, prepared via electropolymerization, offer attractive advantages such as excellent stability, homogeneity, good adhesion to the electrode surface, insolubility, increased surface area, and numerous active sites [16].

Numerous studies have reported the modification of glassy carbon electrode (GCE) surfaces with polymer films for metal ion determination. These polymers typically contain donor atoms (e.g., N, S, and – COOH), which facilitate metal ion binding through electrostatic attraction and significantly enhance complex formation on the electrode surface [7, 9, 16, 17]. The electropolymerization technique provides a simple and efficient method for forming stable polymer films on the electrode surface. Substances such as L-arginine [18], L-cysteine [19], and 2-amino-4-thiazoleacetic acid [20], which are amino acid-based compounds, have been used for polymer electrode modification in the determination of various analytes. These compounds contain functional groups, particularly amine ($–NH_2$) and carboxyl (–COOH) groups. Additionally, some compounds possess specific functional moieties, such as thiol (–SH) groups or heterocyclic rings containing donor atoms (e.g., N or S), which can interact with ions through electrostatic attraction depending on their charge state and promote the formation of coordinate covalent complexes with metal ions. To further improve sensitivity, bismuth film electrodes combined with polymer coatings have been widely applied in ASV for metal ion determination [21–23]. In addition, bismuth-based electrodes generally exhibit low sensitivity to dissolved oxygen (O_2), allowing stripping measurements to be carried out without prior deaeration in many cases [23, 24]. This is attributed to the ability of bismuth to facilitate intermetallic compound formation with target metals, thereby enhancing the stripping response [21]. L-arginine, an amino acid, presents a particularly attractive option for polymer electrode modification due to its cost-effectiveness, environmental friendliness, and ability to form polymer films on GCE surfaces. In addition, poly(L-arginine) contains amine groups ($–NH_2$) that can effectively interact with cations, making it a promising candidate for electrode modification [25].

However, despite extensive research on polymer- and bismuth-modified electrodes, there has been no report on the application of poly(L-arginine) (poly(L-Arg)), which contains guanidinium groups, with bismuth for metal ion determination, particularly Zn(II). This integration can facilitate bismuth–zinc alloy formation during the preconcentration step, thereby enhancing sensitivity and lowering the limit of detection (LOD). Furthermore, its application in real soil samples remains limited. Therefore, this study

aims to develop an environmentally friendly bismuth/poly(L-Arg)-modified glassy carbon electrode (Bi/poly(L-Arg)/GCE) for sensitive Zn(II) determination using anodic stripping voltammetry (ASV), and to evaluate its analytical performance in soil samples from Phuket pineapple plantations. A glassy carbon electrode (GCE) was first modified with poly(L-Arg) via electropolymerization. Subsequently, for Zn(II) determination by ASV, a bismuth film was plated in situ onto the poly(L-Arg)/GCE, resulting in a Bi/poly(L-Arg)/GCE. Optimization of several key operational parameters was conducted, including the L-arginine concentration and the number of electropolymerization cycles for the modified electrode, as well as the Bi(III) concentration, acetate buffer pH, preconcentration potential, and preconcentration time. Furthermore, the analytical performance of the proposed method was evaluated in terms of linear range, LOD, limit of quantitation (LOQ), and repeatability, followed by its application to Zn(II) determination in soil samples.

2 Experimental

2.1 Chemicals and reagents

L-arginine monohydrochloride ($C_6H_{14}N_4O_2 \cdot HCl$, 99.0% purity) was obtained from Loba Chemie (Mumbai, India). Bismuth(III) nitrate pentahydrate ($Bi(NO_3)_3 \cdot 5\ H_2O$, 99.5% purity), dipotassium hydrogen phosphate (K_2HPO_4, 99.0% purity), potassium dihydrogen phosphate (KH_2PO_4, 99.0% purity), sodium acetate trihydrate ($CH_3COONa \cdot 3H_2O$, 99.0% purity), and zinc acetate dihydrate ($Zn(CH_3COO)_2 \cdot 2\ H_2O$, 99.5% purity) were obtained from Ajax Finechem (Taren Point, Australia). Acetic acid (CH_3COOH, 99.7% purity), hydrochloric acid (HCl, 37.0% w/w), hydrogen peroxide (H_2O_2, 30.0% w/w), nitric acid (HNO_3, 65.0% w/w), potassium chloride (KCl, 99.5% purity), potassium ferricyanide ($K_3[Fe(CN)_6]$, 99.0% purity), potassium hydroxide (KOH, 85.0% purity), and sulfuric acid (H_2SO_4, 97.0% purity) were obtained from Merck (Darmstadt, Germany). All solutions were prepared using deionized water (dH_2O, 18.2 MΩ·cm) from a type II water purification system (Model Micra, ELGA, UK).

2.2 Apparatus

All electrochemical measurements were conducted in a conventional three-electrode cell and controlled by a 910 PSTAT mini potentiostat (Metrohm Autolab B.V., The Netherlands). A poly(L-Arg)-modified glassy carbon electrode (GCE; 3.0 mm diameter) served as the working electrode, while a silver/silver chloride (Ag/AgCl, 3 M KCl) electrode and a platinum wire were used as the reference and counter electrodes, respectively. For pH measurements, a SevenCompact™ S220 pH/ion meter (Mettler-Toledo, Switzerland) was employed. The surface morphology of the modified electrode was characterized using scanning electron microscopy (SEM; JSM-5800, JEOL, Japan).

2.3 Procedure

2.3.1 Fabrication of the poly(L-Arg)-modified GCE

Initial electrode preparation involved polishing the working electrode with alumina powders (1.5, 0.5, and 0.05 µm), followed by rinsing with dH_2O. The cleaned electrode then underwent electrochemical activation by cycling the potential from 0.00 to +1.80 V at a scan rate of 0.05 V s^{-1} for 10 cycles in 0.1 mol L^{-1} H_2SO_4, yielding an activated GCE (GCE*). Subsequently, for the poly(L-Arg) electropolymerization, the pretreated GCE* was immersed in 10.0 mmol L^{-1} L-arginine solution in 0.1 mol L^{-1} phosphate buffer (pH 7.0). The electropolymerization procedure was conducted for 10 cycles, scanning from −1.10 to +1.80 V at 0.10 V s^{-1}. After electropolymerization, the resulting poly(L-Arg)/GCE was thoroughly washed with dH_2O and air-dried at room temperature.

2.3.2 ASV measurements

ASV measurements were performed in a 5.0 mL electrochemical cell containing 0.1 mol L^{-1} acetate buffer (pH 5.0). The analytical procedure consisted of two steps. In the preconcentration step, Zn(II) at concentrations of 50–500 µg L^{-1} (for optimization) and Bi(III) at a fixed concentration of 1.0 mg L^{-1} were simultaneously deposited onto the poly(L-Arg)/GCE surface at −1.40 V for 60 s under continuous stirring. Stirring was then ceased for a 5 s equilibration. In the stripping step, Zn(II) was stripped from the poly(L-Arg)/GCE surface. The ASV operating conditions were as follows: preconcentration potential, −1.40 V; preconcentration time, 60 s; amplitude, 0.01 V; frequency, 10.0 Hz; step potential, 0.01 V; potential increment, 0.01 V; and scan range, −1.40 to −0.50 V. Dissolved O_2 was not removed prior to the electrochemical measurements, as no significant interference was observed under the experimental conditions employed.

2.3.3 Sample preparation

Soil samples were collected from a pineapple farm in Baan Manik, Si Sunthon, Thalang District, Phuket, Thailand. Digestion followed US EPA Method 3050B [26]. Each 1.0 g soil sample was first digested with 10.0 mL of 1:1 (v/v) concentrated HNO_3:dH_2O at 95 ± 5 °C for 15 min for

initial oxidation. Additional 5.0 mL aliquots of concentrated HNO_3 were added with heating until brown fumes dissipated, ensuring complete oxidation, and the volume was reduced to ~ 5.0 mL. After cooling, 2.0 mL dH_2O and 3.0 mL 30% H_2O_2 were added. Further 1.0 mL aliquots of H_2O_2 (total ≤ 10.0 mL) were introduced under gentle heat until no further reaction occurred to decompose residual organics, and the solution was again concentrated to ~ 5.0 mL. Finally, 10.0 mL concentrated HCl was added and the mixture was heated at 95 ± 5 °C for 15 min for complete metal oxide dissolution. After cooling, the solution was filtered (Whatman No. 41) and diluted to 100.0 mL with dH_2O. For ASV analysis, the pH of the digests was adjusted to 5.0 with 3.0 mol L^{-1} KOH, and the digests were analyzed directly without further dilution by ASV using the Bi/poly(L-Arg)/GCE and by inductively coupled plasma–optical emission spectrometry (ICP-OES) using a PerkinElmer Optima 8000 DV instrument.

2.4 Use of AI tools in manuscript preparation

No AI tools were used in the experimental work, data analysis, interpretation of the results, or scientific conclusions.

3 Results and discussion

3.1 Electropolymerization and morphological characterization of poly(L-Arg) on GCE

The cyclic voltammograms documented the electropolymerization of poly(L-Arg) on the GCE surface. This process occurred within a potential range − 1.10 to + 1.80 V vs. Ag/AgCl, at a scan rate of 0.10 V s^{-1}, over 10 cycles. The experiment was conducted with a 10.0 mmol L^{-1} L-arginine solution in 0.1 mol L^{-1} phosphate buffer (pH 7.0) (Fig. 1A). The voltammograms showed that the current gradually decreased with each successive scan until the electropolymerization was complete. This observation confirms the deposition of a thin poly(L-Arg) film onto the GCE surface [27].

The surface morphology of the poly(L-Arg)/GCE was characterized using SEM. As shown in Fig. 1B, a bare GCE exhibits a smooth surface, whereas Fig. 1C clearly displays a structured, interconnected, net-like pattern of the poly(L-Arg) film on the GCE surface. This observation confirms the successful formation and adherence of the poly(L-Arg) film on the GCE [28].

3.2 Electrochemical behavior of poly(L-Arg) on GCE

Typically, electrochemical behavior can be evaluated from the relationship between peak current and scan rate or the square root of scan rate, depending on the controlling mechanism. In this study, the electrochemical response of the poly(L-Arg)/GCE was explored using CV with 5.0 mmol L^{-1} $K_3[Fe(CN)_6]$ in 0.1 mol L^{-1} KCl at various scan rates (20–200 mV s^{-1}). As shown in Fig. 2A-B, the well-defined redox peak currents of $K_3[Fe(CN)_6]$ on the poly(L-Arg)/GCE increase with increasing scan rate. To clarify the controlling mechanism, the relationships of both anodic ($I_{p.a.}$) and cathodic (I_{pc}) peak currents with scan rate (ν) and the square root of scan rate ($\nu^{1/2}$) were examined. The $I_{p.a.}$ and I_{pc} show a linear dependence on the square root of scan rate, as described by the following regression equations:

$$I_{pa}(\mu A) = (12.30 \pm 0.04)\,\nu^{1/2} + (3.5 \pm 0.6)\,; R^2 = 0.9998$$

$$I_{pc}(\mu A) = (-12.49 \pm 0.04)\,\nu^{1/2} - (1.2 \pm 0.6)\,; R^2 = 0.9998$$

The linear dependence of the peak currents on $\nu^{1/2}$ indicates that the ferri/ferrocyanide ($[Fe(CN)_6]^{3-/4-}$) redox process at the poly(L-Arg)/GCE is diffusion-controlled rather.

than adsorption-controlled [29, 30]. As shown in Fig. 2C, the cyclic voltammograms show.

the redox peaks of $K_3[Fe(CN)_6]$ on both the bare GCE and the poly(L-Arg)/GCE, with the poly(L-Arg)/GCE exhibiting a notably higher response than the bare GCE. Specifically, anodic peak potential (E_{pa}) was observed at + 0.35 V for poly(L-Arg)/GCE and + 0.45 V for bare.

GCE (vs. Ag/AgCl), while the cathodic peak potential (E_{pc}) was observed at + 0.25 V for poly(L-Arg)/GCE and + 0.15 V for bare GCE (vs. Ag/AgCl). The peak-to-peak separation (ΔE_p) for the poly(L-Arg)/GCE is 0.10 V, which is lower than that of the bare GCE (0.30 V), indicating improved electron-transfer kinetics upon modification. Peak currents were quantified and, where appropriate, interpreted using the Randles-Ševčík Eqs [29, 30].

$$I_{pa} = 2.69 \times 10^5 n^{3/2} A_0 D_0^{1/2} \upsilon^{1/2}$$

where $I_{p.a.}$ is the anodic peak current, n is the number of electrons transferred, A_0 is the electroactive electrode area (cm^2), D_0 is the diffusion coefficient of $[Fe(CN)_6]^{3-/4-}$ (7.6×10^{-6} cm^2 s^{-1}), C_0 is the concentration of $K_3[Fe(CN)_6]$ (mol cm^{-3}), and υ is the scan rate in V s^{-1}. The electroactive surface areas were estimated from the slopes of the $I_{p.a.}$ versus $\nu^{1/2}$ plots using the Randles-Ševčík equation. The electroactive surface areas of poly(L-Arg)/GCE and the bare GCE were determined to be 0.13 cm^2 and 0.08 cm^2, respectively. Notably, the poly(L-Arg)/GCE exhibits an

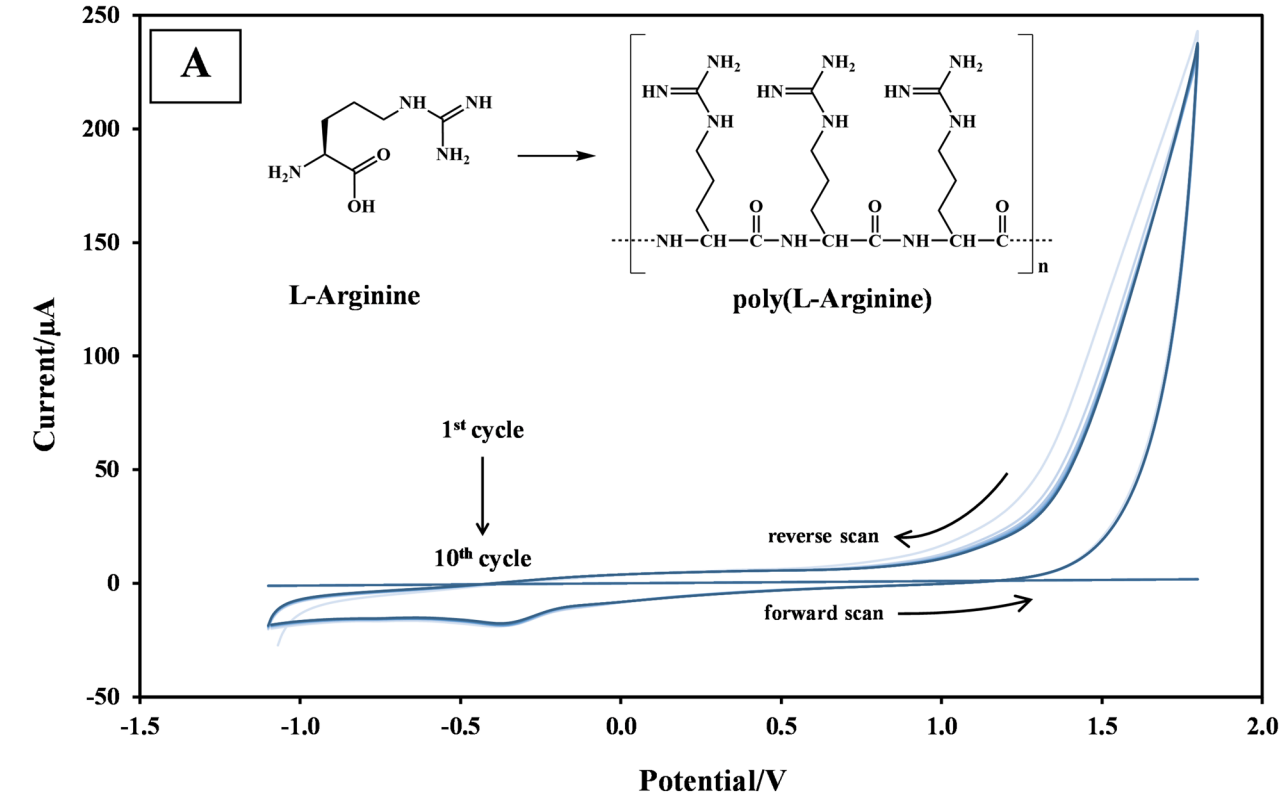

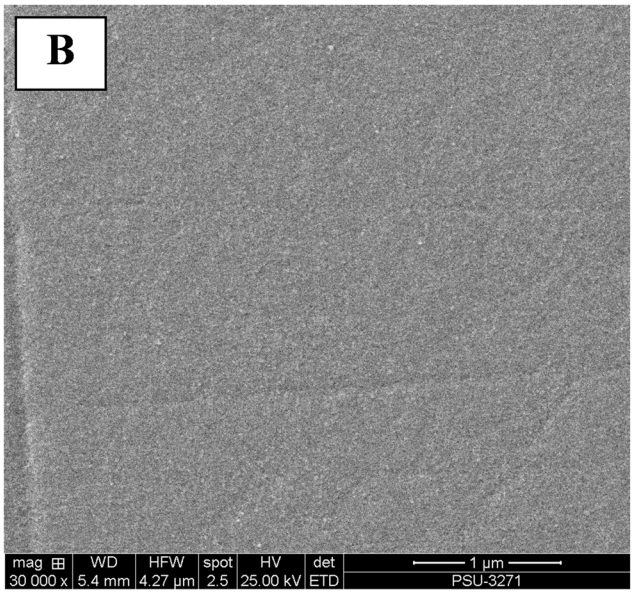

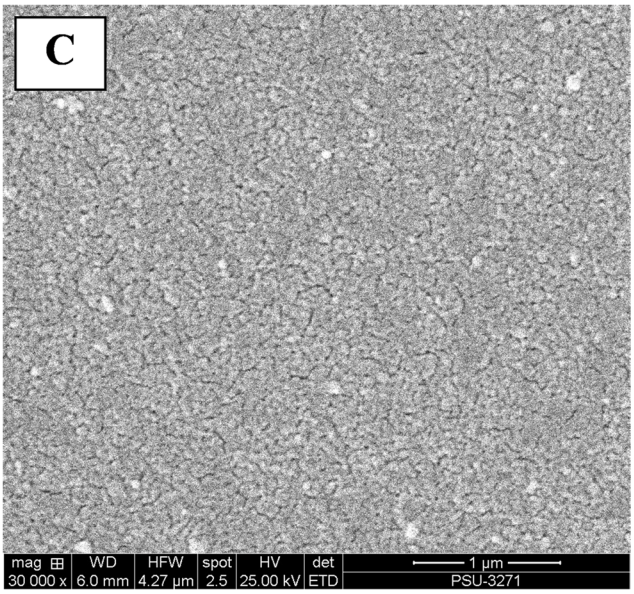

Fig. 1 **A** Cyclic voltammograms recorded during the electropolymerization of poly(L-Arg) on a GCE in 10.0 mmol L^{-1} L-arginine (0.1 mol L^{-1} phosphate buffer, pH 7.0); potential window − 1.10 to + 1.80 V vs. Ag/AgCl; scan rate 0.10 V s^{-1}; 10 cycles. The voltammograms represent successive scans; the 1st and 10th cycles are indicated in the figure, and the scan direction is shown by arrows. **B** An SEM image shows a bare GCE (30,000×). **C** An SEM image shows the poly(L-Arg) film showing an interconnected, net-like morphology on the GCE surface

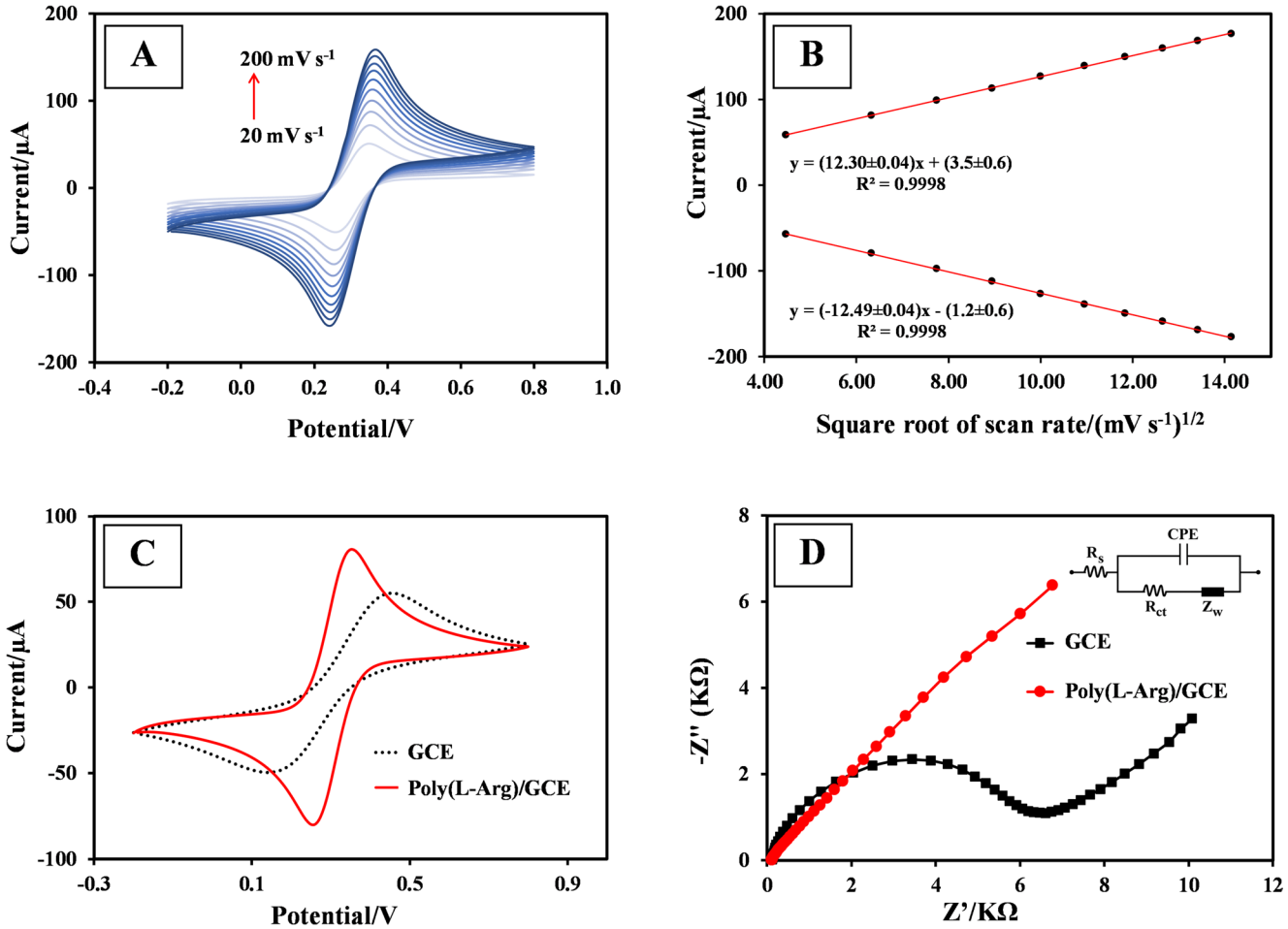

Fig. 2 Electrochemical behavior of the poly(L-Arg)/GCE. **A** Cyclic voltammograms of 5 mmol L^{-1} $K_3[Fe(CN)_6]$ in 0.1 mol L^{-1} KCl recorded on the poly(L-Arg)/GCE at scan rates of 20–200 mV s^{-1}. **B** Linear relationships of $I_{p.a.}$ and I_{pc} versus the square root of scan rate. **C** Comparison of cyclic voltammograms of 5.0 mmol L^{-1} $K_3[Fe(CN)_6]$ (0.1 mol L^{-1} KCl) at the bare GCE and the poly(L-Arg)/GCE. **D** EIS results for the bare GCE and the poly(L-Arg)/GCE recorded in 5.0 mmol L^{-1} $K_3[Fe(CN)_6]$ (0.1 mol L^{-1} KCl; 0.01–100 kHz)

approximately 1.62-fold higher electroactive surface area than the bare GCE.

This observation confirms that the enhanced electroactive surface area of the poly(L-Arg) film contributes to the improved electrochemical response of the modified electrode compared to the bare GCE. Furthermore, the electrochemical behaviors of both the bare GCE and.

poly(L-Arg)/GCE were explored using electrochemical impedance spectroscopy (EIS). In this study, EIS measurements were conducted on both the bare GCE and poly(L-Arg)/GCE within a frequency range of 0.01–100 kHz. These measurements were performed in a solution containing 5.0 mmol L^{-1} $[Fe(CN)_6]^{3-/4-}$ in 0.1 mol L^{-1} KCl. The EIS data were fitted to the equivalent circuit Rs(CPE(RctZw)), and the charge transfer resistance (Rct) values were obtained from the fitted parameters for spectra exhibiting a discernible semicircular feature. Figure 2D illustrates the resulting Nyquist plots. The bare GCE exhibited a large semicircle, and the fitted result gave an Rct value of 6.93 ± 0.05 kΩ, indicating sluggish electron transfer during the $[Fe(CN)_6]^{3-/4-}$ redox reaction. In contrast, the poly(L-Arg)/GCE showed a nearly linear Nyquist response, suggesting reduced interfacial impedance and enhanced electron transfer after electrode modification. Such a nearly linear Nyquist response may be qualitatively associated with diffusion-related impedance behavior, particularly in the low-frequency region where the impedance response is influenced by the Warburg diffusion element, whereas the diminished semicircular component generally indicates a lower charge-transfer resistance and improved electron-transfer kinetics at the modified electrode surface [31, 32]. Because no discernible semicircle was observed for the poly(L-Arg)/GCE, a reliable Rct value could not be obtained, and the EIS response was therefore discussed qualitatively.

3.3 Comparison of GCE, Bi/GCE, poly(L-Arg)/GCE, and Bi/poly(L-Arg)/GCE for Zn(II) detection using anodic stripping voltammetry

For various electrode modifications, the sensitivity was determined from the slope of the calibration curve, which correlates the oxidation peak current with Zn(II) concentration. These calibration plots, ranging from 50 to 500 µg L^{-1} Zn(II) in a 0.10 mol L^{-1} acetate buffer.

(pH 4.5), are shown in Fig. 3. The sensitivity of Zn(II) at the Bi/poly(L-Arg)/GCE was 27.2, 1.8, and 1.7 times higher than that at the bare GCE, Bi/GCE, and poly(L-Arg)/GCE, respectively. These results suggest that the high anodic peak current at the Bi/poly(L-Arg)/GCE is attributed to the adsorption of Zn(II) onto the amine groups ($–NH_2$) within the poly(L-Arg) molecule on the GCE surface via a coordinate covalent bond [25]. Additionally, the formation of a bismuth-zinc (Bi–Zn) alloy further contributes to the observed peak current enhancement [33, 34].

3.4 Optimization of the fabrications of poly(L-Arg)/GCE

3.4.1 Effect of L-arginine concentration

The effect of L-arginine concentration, ranging from 1.0 to 20.0 mmol L^{-1}, was investigated for the electropolymerization of poly(L-Arg) on the GCE surface. Experiments were conducted in 0.1 mol L^{-1} phosphate buffer (pH 7.0) using ten scans at a scan rate of 0.10 V s^{-1} within the potential range of −1.10 to +1.80 V. As shown in Fig. S1A, Zn(II) and Bi(III) were simultaneously deposited onto the poly(L-Arg)/GCE surface at −1.40 V for 60 s. The sensitivity of Zn(II) detection exhibited an initial increase within the 1.0–10.0 mmol L^{-1}.

L-arginine range. This increase is attributed to the enhanced availability of active ligand sites on the GCE surface, including oxygen and nitrogen atoms, which facilitate complex formation with zinc [35, 36]. However, when L-arginine concentrations exceeded 10.0 mmol L^{-1}, the sensitivity of Zn(II) decreased. This phenomenon was attributed to the formation of an excessively thick poly(L-Arg) film on the GCE surface, which impedes electron transfer. Consequently, 10.0 mmol L^{-1} L-arginine was selected for further experiments [37].

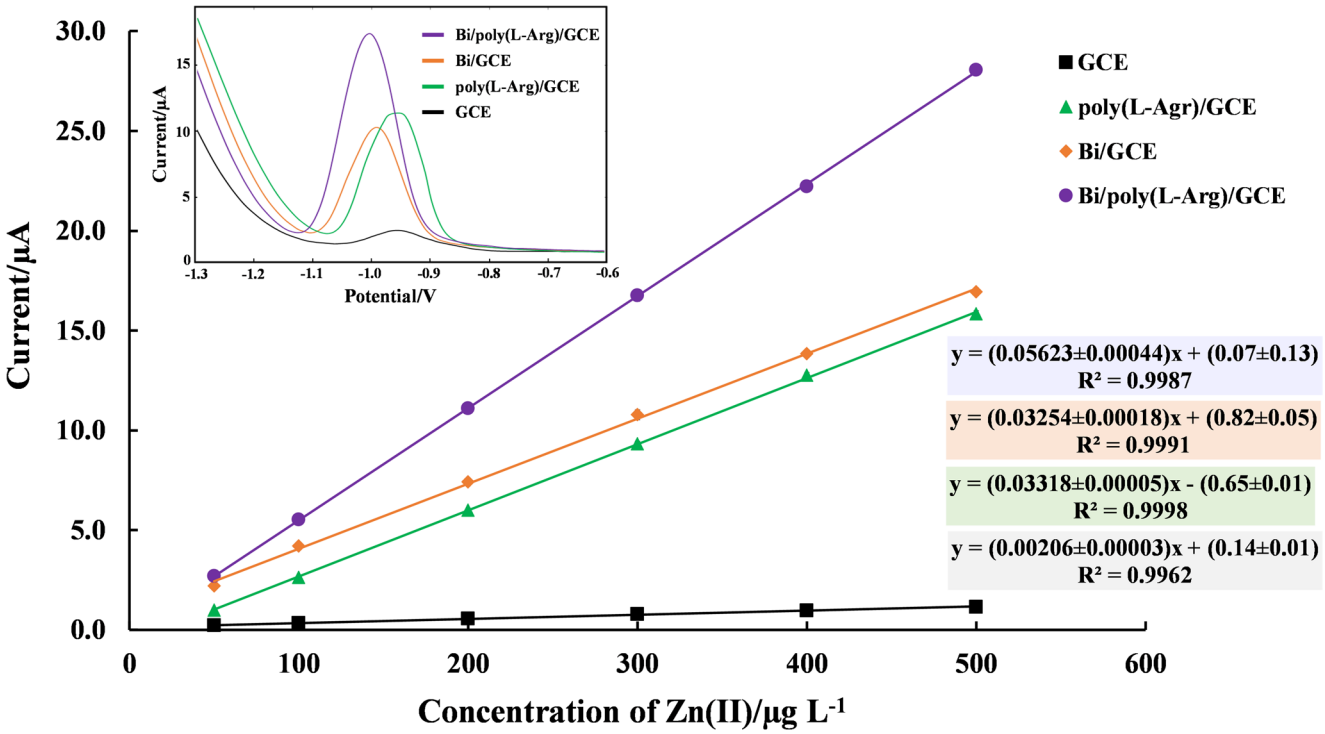

Fig. 3 Comparison of the analytical performance of GCE, poly(L-Arg)/GCE, Bi/GCE, and Bi/poly(L-Arg)/GCE for Zn(II) detection. Calibration plots of stripping peak current versus Zn(II) concentration (50–500 µg L^{-1}) with the corresponding regression lines used to determine sensitivity. Inset: Anodic stripping voltammograms of all electrodes recorded at the same Zn(II) concentration (300 µg L^{-1}). Measurements were performed in 0.10 mol L^{-1} acetate buffer (pH 4.5). ASV operating conditions: preconcentration potential, −1.40 V; preconcentration time, 60 s; and a square-wave potential scan from −1.40 to −0.50 V

3.4.2 Effect of the number of cyclic voltammetric scans of poly(L-Arg) on the GCE surface

The effect of number of cyclic voltammetric scans on the electropolymerization of poly(L-Arg) on the GCE surface was studied. Experiments were conducted using 10.0 mmol L^{-1}.

L-arginine at a scan rate of 0.10 V s^{-1} within a potential range of − 1.10 to + 1.80 V, with the number of cycles varying from 5 to 20. The results are shown in Fig. S1B. The sensitivity of Zn(II) detection initially increased with the number of cycles ranging from 5 to 10 cycles, due to the increasing number of active ligand sites [33]. However, when the number of cycles exceeded 10, the sensitivity of Zn(II) decreased, possibly due to an excessively thick poly(L-Arg) film on the GCE surface that impedes electron transfer [37]. Therefore, 10 cyclic voltammetric scans for poly(L-Arg) electropolymerization on the GCE surface were selected for further experiments.

Furthermore, the sensitivity of Zn(II) detection at L-arginine concentrations of 7.5 and 12.5 mmol L^{-1} was also examined with a varying numbers of cyclic voltammetric scans for electropolymerization on GCE surface, as shown in Fig. S1C. The numerically highest sensitivity for Zn(II) detection was observed at 12.5 mmol L^{-1} L-arginine and 7 cyclic voltammetric scans. However, the sensitivity obtained at 10.0 mmol L^{-1} L-arginine and 10 scans was very similar (0.05623 vs. 0.05628 µA (µg L^{-1})$^{-1}$). Therefore, 10.0 mmol L^{-1}.

L-arginine and 10 cyclic voltammetric scans for poly(L-Arg) electropolymerization on the GCE surface were selected for further experiments, because they provided practically comparable analytical performance while requiring a lower L-arginine concentration, thereby reducing chemical consumption and better supporting the green-chemistry concept [29].

3.5 Optimization of the operational conditions for zinc detection by anodic stripping voltammetry at the Bi/poly(L-Arg)/GCE

3.5.1 Effect of bismuth concentration

The Bi(III) concentration for in situ plating on the poly(L-Arg)/GCE was investigated for Zn(II) detection by ASV technique, ranging from 0.1 to 2.0 mg L^{-1} Bi(III). Zn(II) and Bi(III) were simultaneously deposited onto the poly(L-Arg)/GCE surface at − 1.40 V for 60 s in 0.1 mol L^{-1} acetate buffer (pH 4.5), as shown in Fig. S2 (A). The sensitivity of Zn(II) detection initially increased within 0.1–1.0 mg L^{-1} Bi(III) concentration. This increase is attributed to greater Bi film deposition on the poly(L-Arg)/GCE, which resulted in increased Bi-Zn alloy formation on the electrode surface and, consequently, an elevated anodic peak current. However, when the Bi(III) concentration exceeded 1.0 mg L^{-1}, the sensitivity of Zn(II) decreased. This phenomenon may be attributed to the Bi film on the poly(L-Arg)/GCE surface becoming excessively thick, which in turn inhibits Zn(II) adsorption and thereby decreases the anodic peak current during the stripping step [38]. In the present study, the stripping response increased with Bi(III) concentration up to 1.0 mg L^{-1}, whereas a further increase in Bi(III) concentration led to a decrease in signal, consistent with the formation of an excessively thick bismuth layer on the poly(L-Arg)/GCE surface [39]. Therefore, 1.0 mg L^{-1} Bi(III) was selected for further experiments, while the calculated apparent surface coverage (Γ) values are provided in the Supporting Information (Table S1).

3.5.2 Effect of the pH of the acetate buffer solution

The effect of pH of a 0.1 mol L^{-1} acetate buffer solution on Zn(II) detection was studied in the range of pH 4.0–6.0, as shown in Fig. S2 (B). The sensitivity of Zn(II) detection initially increased within the pH 4.0–5.0, but decreased when the pH was higher than 5.0. This behavior is attributed to the availability of oxygen and nitrogen donor sites (from the hydroxyl, –OH, and amine, $–NH_2$, groups) within the poly(L-Arg) film on the poly(L-Arg)/GCE surface, which facilitate the adsorption of Zn(II) via coordinate covalent bonds [25]. At a pH lower than 5.0, a decrease in Zn(II) detection sensitivity was observed. This may be attributed to the electrostatic repulsion between the protonated polymer and the metallic cation. Conversely, at a pH higher than 5.0, the sensitivity of Zn(II) detection also decreased, possibly due to the formation of hydroxide precipitates, specifically zinc hydroxide ($Zn(OH)_2$), thereby reducing the amount of Zn(II) in solution [16]. Therefore, 0.1 mol L^{-1} acetate buffer at pH 5.0 was selected for further experiments.

3.5.3 Effect of the acetate buffer solution's concentration at pH 5.0

The effects of acetate buffer concentration at pH 5.0 on Zn(II) detection were investigated over the range 0.05–0.20 mol L^{-1} as shown in Fig. S2(C). The sensitivity of Zn(II) detection increased initially in the range 0.05–0.10 mol L^{-1}, but decreased when acetate concentration was higher than 0.10 mol L^{-1}. This decrease is more plausibly attributed to increased complexation of Zn(II) with acetate at higher acetate levels, which shifts Zn(II) from free/electroactive forms to acetate-bound species and thereby lowers the fraction available for preconcentration [40, 41] Conversely, acetate concentrations below 0.10 mol L^{-1} likely provided

insufficient supporting electrolyte, which can increase solution resistance and ohmic (iR) drop and reduce the suppression of ionic migration, thereby lowering the measured anodic peak current [42]. Therefore, 0.1 mol L^{-1} acetate buffer solution at pH 5.0 was selected for further experiments.

3.5.4 Effect of the preconcentration potential

The effect of the preconcentration potential on Zn(II) detection sensitivity at the Bi/poly(L-Arg)/GCE was investigated, ranging from − 1.30 to − 1.70 V at a preconcentration time of 60 s, as shown in Fig. S2 (D). The Sensitivity of Zn(II) detection initially increased within the − 1.30 to − 1.50 V range. However, at potentials more negative than − 1.50 V, it decreased, due to enhanced hydrogen evolution at the electrode surface, where the generated hydrogen gas might inhibit Zn(II) adsorption [16, 43]. Conversely, preconcentration potentials less negative than − 1.50 V were insufficient to stimulate Zn(II) reduction, resulting in a decreased anodic peak current during the stripping step. Therefore, a preconcentration potential of − 1.50 V was selected for further experiments.

3.5.5 Effect of the preconcentration time

The effect of preconcentration time on Zn(II) detection sensitivity at the.

Bi/poly(L-Arg)/GCE was investigated, ranging from 30 to 300 s at a preconcentration potential of − 1.50 V, as shown in Fig. S2 (E). The Sensitivity initially increased within the 30–150 s range. However, beyond 150 s, it remained essentially constant or showed only a slight change, probably due to saturation of Zn(II) on the poly(L-Arg)/GCE surface [16, 44]. Therefore, a preconcentration time of 150 s was selected for further experiments, as this condition provides high analytical sensitivity while keeping the analysis time short.

In summary, the optimum conditions for fabricating poly(L-Arg)/GCE were 10.0 mmol L^{-1} L-arginine and 10 cyclic voltammetric scans. Subsequently, the optimal operational parameters for Zn(II) detection by ASV were established as 1.0 mg L^{-1} Bi(III), 0.10 mol L^{-1} acetate buffer at pH 5.0, a preconcentration time of 150 s, and a preconcentration potential of − 1.50 V.

3.6 Performances of the Bi/poly(L-Arg)/GCE for zinc detection by ASV

3.6.1 Calibration curve, LOD, and LOQ

Following the determination of optimal conditions for both poly(L-Arg)/GCE fabrication and Zn(II) detection via the bismuth-coated ASV technique, a calibration study was performed. A calibration curve was generated for Zn(II) concentrations in the range of 7.5–400 µg L^{-1}, as shown in Fig. 4. The anodic peak current of Zn(II) at the Bi/poly(L-Arg)/GCE was observed at a potential of − 1.04 V (vs. Ag/AgCl). The linear regression equation for Zn(II) was determined to be $i_p = (0.1153 \pm 0.0030)x - (1.11 \pm 0.03)$ (r = 0.999), where x is the Zn(II) concentration in µg L^{-1}. The observed negative intercept is attributed to a small residual background/baseline offset at zero analyte concentration, rather than to poor linearity of the analytical method. Consequently, the regression was not forced through the origin, and the full calibration equation was retained for quantification. The sensitivity, defined as the slope of the regression equation, was 0.1153 ± 0.0030 µA (µg L^{-1})$^{-1}$. The calculated limit of detection (LOD) and limit of quantification (LOQ) were 0.78 and 2.6 µg L^{-1}, respectively, obtained using the equations $LOD = 3S_a/b$ and $LOQ = 10S_a/b$, where S_a is the standard deviation of the intercept and b is the slope of the calibration curve [45]. Based on the sample preparation procedure, these values correspond to 0.078 and 0.26 mg kg^{-1} on a soil basis, respectively. These values are both below the lower limit of the linear range, confirming the consistency of the analytical performance of the proposed method.

All linear ranges and LOD values are expressed in µg L^{-1} for comparison. Values originally reported in molar concentration or other concentration units were converted to µg L^{-1} using the molar mass of Zn (65.38 g mol^{-1}), where appropriate. BiFE, bismuth film electrode; DPASV, differential pulse anodic stripping voltammetry; ASV, anodic stripping voltammetry; SWASV, square-wave anodic stripping voltammetry; DPV, differential pulse voltammetry; SWV, square-wave voltammetry; LOD, limit of detection.

In Table 1, the analytical performance of the proposed Bi/poly(L-Arg)/GCE sensor is compared with previously reported electrochemical Zn(II) sensors. Direct comparison should be made with caution because the reported systems differ in electrode materials, voltammetric techniques, and sample matrices. The literature sensors exhibit a wide range of LODs and linear ranges depending on the electrode material, sensing platform, and analytical conditions. Among the sensors summarized in Table 1, the HDPBA-MWCNT/CPE sensor had the lowest LOD among the listed sensors (0.162 µg L^{-1}), whereas BiFE and Bi-In/GCE exhibited LOD values of 2.95 and 2.3 µg L^{-1}, respectively. However, some of these systems involve more elaborate electrode modification procedures and/or were demonstrated in different sample matrices. In comparison, the Bi/poly(L-Arg)/GCE developed in this work achieved an LOD of 0.78 µg L^{-1} using a convenient ASV protocol. Its linear range (7.5–400 µg L^{-1}) is suitable for environmentally relevant Zn(II)

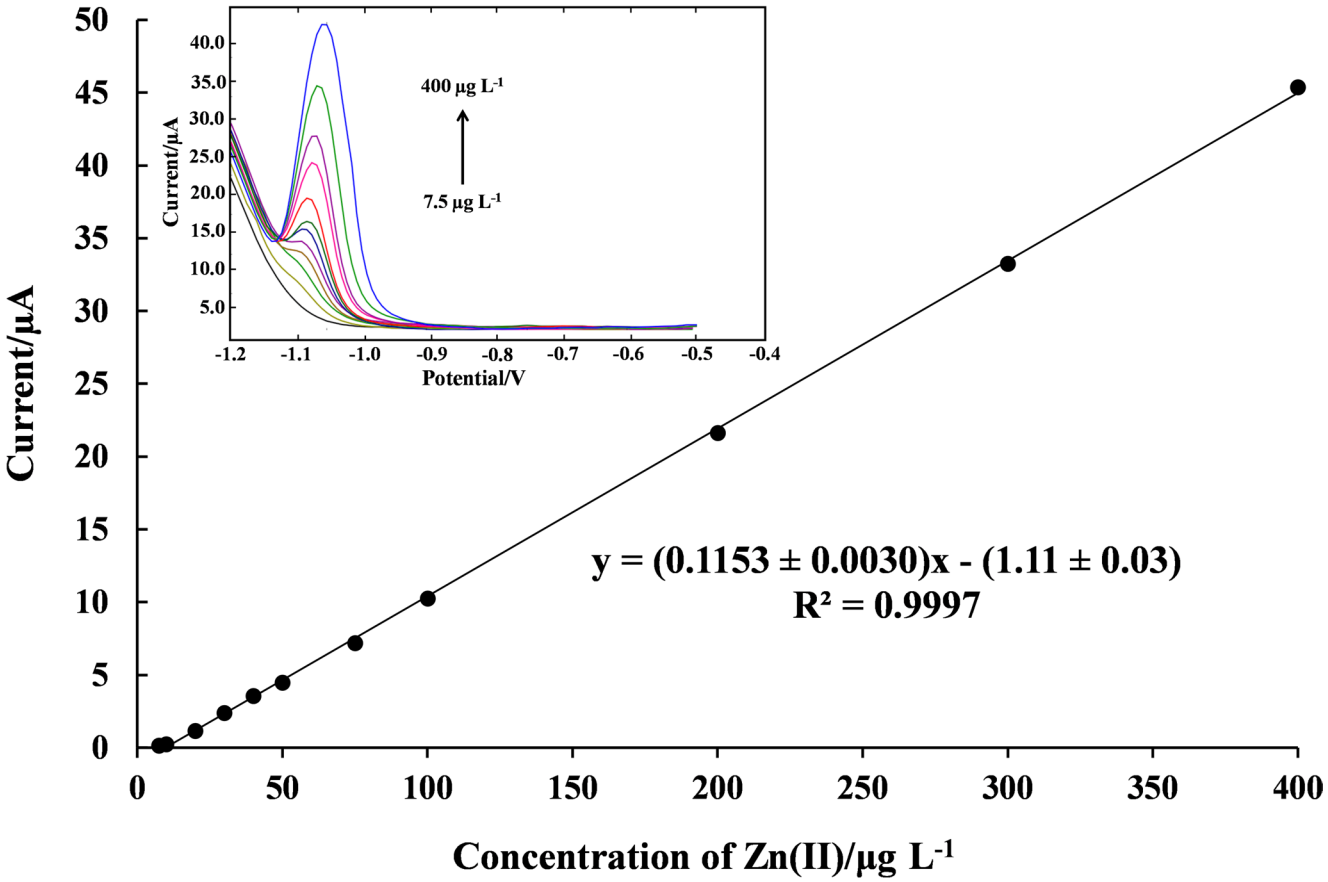

Fig. 4 The calibration curve for Zn(II) showing the linear relationship between the anodic peak current and analyte concentration from 7.5–400 μg L^{-1}. The inset displays the corresponding anodic stripping voltammograms. ASV operating conditions: preconcentration potential of − 1.50 V, a preconcentration time of 150 s, and a square-wave potential scan from − 1.20 to − 0.50 V

Table 1 Comparison of the analytical performance of the proposed Bi/poly(L-Arg)/GCE with previously reported electrochemical Zn(II) sensors

No.	Electrode / sensor	Technique	Linear range (μg L^{-1})	LOD (μg L^{-1})	Sample / application	References
1	BiFE	DPASV	5–110	2.95	water samples	[46]
2	Bi/GO/GCE	ASV	20–8000	6	Seminal fluid	[47]
3	Bi–In/GCE	ASV	2.5–500	2.3	Krebs buffer	[48]
4	HDPBA-MWCNT/CPE	SWASV	1.31–653.8	0.162	Water samples	[14]
5	f-MWCNT/CS/PB/Au	DPV	200–7000	17.0	Drinking water	[49]
6	Zincon/CNT	SWV	125–1000	20 (saliva) 30 (urine)	Urine / saliva	[50]
7	G/HNFQ/CPE	SWV	30.7–6133	18.3	River water	[51]
8	Bi/poly(L-Arg)/GCE	ASV	7.5–400	0.78	Phuket pineapple cultivation soil	This work

levels, and its successful application to Phuket pineapple cultivation soil samples demonstrates its practical utility.

3.6.2 Repeatability

The repeatability of the Bi/poly(L-Arg)/GCE sensor (intra-electrode repeatability) was first assessed using a single electrode. Measurements were performed on standard Zn(II) solutions of 50–400 μg L^{-1} using ASV, with three replicate determinations at each concentration (n = 3), giving a total of 18 measurements, as shown in Fig. 5A. Additionally, the inter-electrode reproducibility of six independently fabricated Bi/poly(L-Arg)/GCE electrodes was assessed at each Zn(II) concentration, as shown in Fig. 5B. Both the single electrode and the six fabricated electrodes demonstrated good intra-electrode repeatability and inter-electrode reproducibility, respectively. The relative standard deviation (RSDs) for the single electrode ranged from 1.5% to 9.8%, while those across six electrodes ranged from 0.6% to 4.1%. These results meet the requirements of the AOAC Official

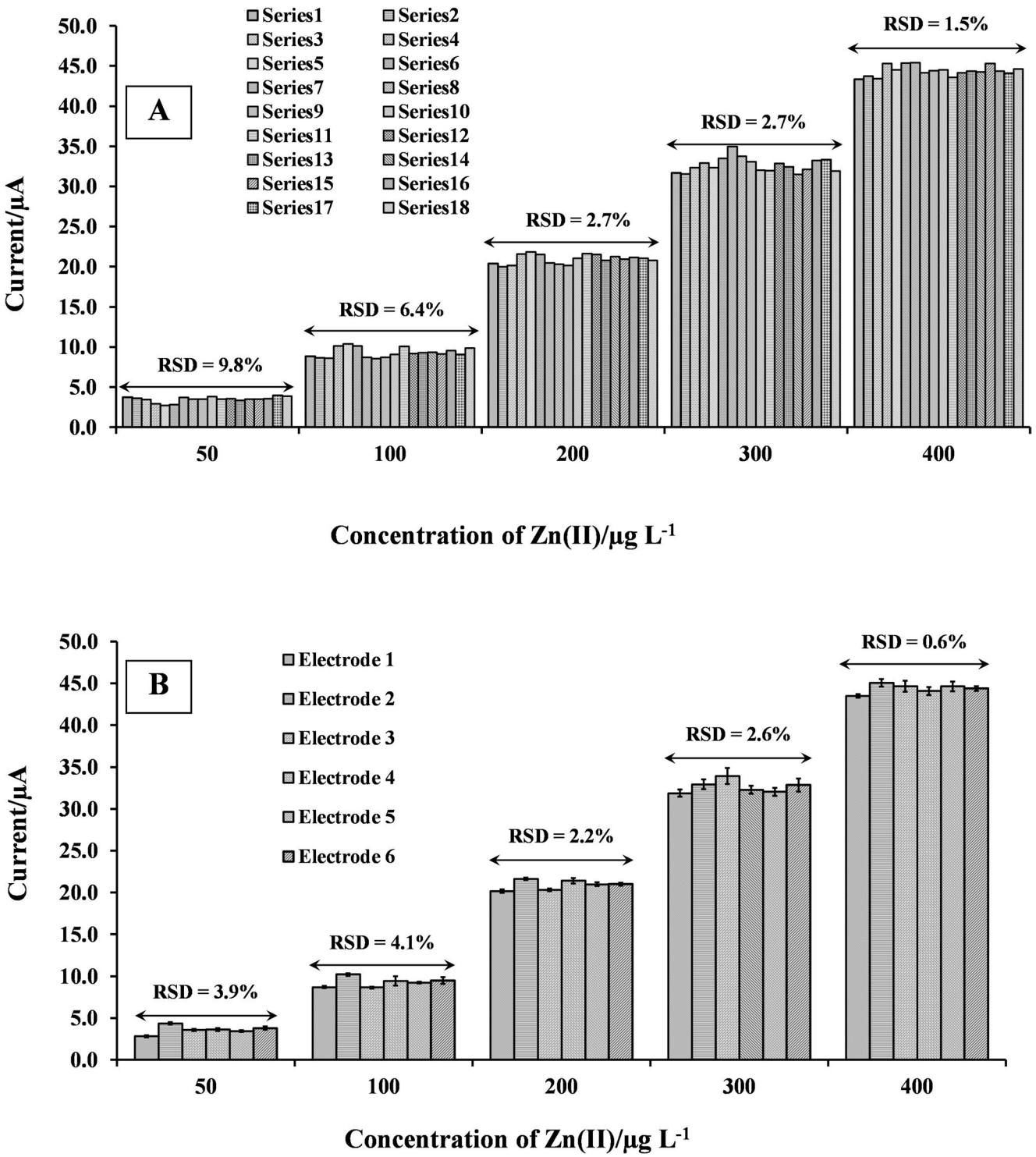

Fig. 5 Precision of Zn(II) detection using the Bi/poly(L-Arg)/GCE. Measurements were performed on standard Zn(II) solutions in the range of 50–400 µg L^{-1}. **A** Intra-electrode repeatability, evaluated using a single electrode with three replicate measurements at each concentration. **B** Reproducibility (inter-electrode across six independently prepared electrodes; replicate measurements per electrode). Results are expressed as mean ± SD; RSD values are given in %

Table 2 Determination of zinc content and recovery in Phuket pineapple-cultivation soils by ASV using the Bi/poly(L-Arg)/GCE and comparison with ICP-OES

Sample	ICP-OES (mg kg^{-1})	Proposed method (mg kg^{-1})	% Recovery (proposed method) Spiked Concentration (mg kg^{-1})		
			0.05	0.30	0.50
1	0.980 ± 0.002	1.00 ± 0.20	86 ± 2	91.0 ± 0.3	88.3 ± 0.3
2	1.020 ± 0.005	1.00 ± 0.30	93 ± 2	90 ± 1	88.2 ± 0.2
3	0.850 ± 0.007	0.80 ± 0.10	84 ± 7	93 ± 2	90 ± 1
4	0.550 ± 0.001	0.50 ± 0.20	94 ± 3	93 ± 2	94.7 ± 0.6
5	0.780 ± 0.001	0.80 ± 0.10	90 ± 9	92 ± 2	90.4 ± 0.5
6	0.880 ± 0.005	0.87 ± 0.05	90 ± 8	90 ± 1	91 ± 1

Methods of Analysis criterion of ≤ 15% repeatability at 0.1 mg L^{-1} (100 µg L^{-1}) [52].

3.6.3 Interference study

The influence of coexisting ions on Zn(II) detection was evaluated by adding Cd(II), Cu(II), Fe(III), Pb(II), Mn(II), and Mg(II) to the Zn(II) solution under the optimized conditions. Using a tolerance criterion of 95–105% of the Zn(II) signal obtained in the absence of the interferent, Cd(II), Cu(II), Fe(III), Mn(II), and Mg(II) were tolerated up to Zn: interferent ratios of 1:6, 1:3, 1:7, 1:3, and 1:2, respectively, whereas Pb(II) caused pronounced interference even at a 1:1 ratio. These results indicate that the proposed sensor has limited tolerance toward some coexisting ions, particularly Pb(II). Nevertheless, the matrix-matched calibration results and the agreement with ICP-OES suggest that such interference was not severe under the conditions of the tested soil samples. The detailed interference data are provided in Table S2.

3.7 Determination of zinc in Phuket pineapple cultivation soil samples

The effects of matrix components in real soil samples on the anodic peak current were investigated to evaluate the performance of the developed Bi/poly(L-Arg)/GCE. This study was conducted under the optimized conditions by comparing the response from a standard calibration curve with matrix-matched calibration curves. The slopes of the standard and matrix-matched calibration curves for all real samples were not significantly different at a 95% confidence level ($P > 0.05$). This indicated that matrix components in the soil samples do not significantly affect Zn(II) determination by ASV using the Bi/poly(L-Arg)/GCE. Since the matrix effects were negligible, the standard calibration curve was used directly for Zn(II) quantification in real soil samples. The zinc content in six Phuket pineapple cultivation soils ranged from 0.50 to 1.00 mg kg^{-1}, as determined by ASV using the Bi/poly(L-Arg)/GCE. Statistical analysis using the Wilcoxon Signed-Rank test at a 95% confidence level ($P > 0.05$) showed no significant difference compared with the standard method (ICP-OES), as detailed in Table 2. Although no significant difference in the mean Zn concentrations was observed between ASV and ICP-OES, the SW-ASV measurements showed higher relative variability in some cases, likely because electrochemical stripping measurements are more sensitive to small variations in electrode surface condition, in situ Bi-film formation, solution composition, and matrix-related effects [42]. By contrast, ICP-OES is a laboratory-based instrumental reference method operated under highly controlled conditions, and therefore typically exhibits lower signal dispersion and better precision [53]. Additionally, recovery was evaluated by standard addition under the optimized conditions. For clarity, the added Zn(II) levels are reported in Table 2 as equivalent spiked concentrations of 0.05, 0.30, and 0.50 mg kg^{-1} on a soil basis. The recoveries were 84.1–94.7%, which is consistent with the AOAC Official Methods of Analysis requirements of 80–110% for recoveries at the 0.1 mg kg^{-1} level [52, 54], These results are presented in Table 2.

An investigation of six soil samples from Phuket pineapple plantations revealed Zn concentrations of 0.50–1.00 mg kg^{-1}. These levels are generally considered sufficient for most plant requirements, which typically fall between 0.5 and 3.0 mg kg^{-1}. Although some samples (specifically 3, 4, 5, and 6) showed relatively low Zn concentrations, all remained above the critical deficiency level of 0.5 mg kg^{-1}. However, considering the specific Zn requirements for pineapple (ideally 3 mg kg^{-1}), the Zn concentrations in all studied soil samples are below the optimal threshold for pineapple cultivation. These findings highlighted the needs for Zn supplementation in these soils to promote optimal growth and maximize pineapple yield.

Zinc supplementation can be effectively achieved using zinc sulphate heptahydrate ($ZnSO_4 \cdot 7H_2O$), a highly soluble compound readily absorbed by plants. This can be applied either to the soil or as a foliar spray. For soil application, 30 kg ha^{-1} can be incorporated into previously uncultivated soils, with repeat applications may be necessary in very light sandy soils under replant conditions. Alternatively, for foliar application, a rate of 2 kg per 2,000 L of water per hectare, applied twice with a one-month interval, is sufficient to correct deficiency symptoms [4].

4 Conclusions

An environmentally friendly Bi/poly(L-Arg)/GCE was successfully developed for the voltammetric determination of Zn(II) in soils, with particular relevance to agricultural

monitoring, specifically for measuring zinc in Phuket pineapple cultivation soils. The glassy carbon electrode was first modified by electropolymerizing poly(L-arginine) and then coated in situ with a bismuth film, yielding a composite surface that enabled sensitive and reliable anodic stripping voltammetry measurements. Operating parameters—including L-arginine concentration and electropolymerization cycles, Bi(III) concentration, acetate buffer pH, and the preconcentration potential and time—were systematically optimized to achieve optimal analytical performance. Under the optimized conditions, the method demonstrated excellent analytical characteristics, providing a linear response over 7.5–400 μg L^{-1} ($r = 0.999$), with a limit of detection of 0.78 μg L^{-1} and a limit of quantitation of 2.6 μg L^{-1}. The sensor successfully delivered accurate and reproducible Zn(II) determinations in soil samples from Phuket pineapple plantations, affording recoveries of 84.1–94.7%, and its results were in good agreement with those obtained by ICP-OES, confirming the method's reliability. The mercury-free Bi film and the aminated poly(L-Arg) interface collectively provide high sensitivity, reduced reagent consumption, and operational simplicity, while also offering a low-toxicity and environmentally friendly alternative due to the elimination of hazardous mercury and minimized chemical usage, in line with the principles of green chemistry. These features indicate that the proposed approach is well suited for routine, on-site monitoring of Zn(II) in agricultural soils and has strong potential for deployment in portable electrochemical instrumentation.

Supplementary Information The online version contains supplementary material available at https://doi.org/10.1007/s10800-026-02511-5.

Acknowledgements The authors gratefully acknowledge the Department of Chemistry, Faculty of Science and Technology, Phuket Rajabhat University, for facilitating this research and providing laboratory facilities, and Mr. Wichai Saetan for supplying soil samples from Phuket pineapple plantations for this study, and Assoc. Prof. Dr. Wendy S. Nielsen for writing, reviewing, and editing.

Author contributions A.D.: Conceptualization; Methodology; Investigation; Formal analysis; Writing – original draft; Writing – review & editing; Project administration; Corresponding author.S.C.: Methodology; Resources; Writing – review & editing.S.D.: Validation.W.L.: Methodology; Supervision; Resources; Writing – review & editing.S.P.: Visualization; Resources; Writing – review & editing; Corresponding author.

Funding This work was supported by a research grant from Phuket Rajabhat University.

Data availability The data that support the findings of this study are available from the corresponding author upon reasonable request.

Declarations

Conflict of interest The authors declare no competing interests.

Declaration regarding the use of AI During the preparation of this manuscript, the authors used AI-assisted language editing tools solely to improve grammar and readability. No AI tools were used to generate scientific content, experimental data, data analysis, interpretation of the results, or scientific conclusions. The authors carefully reviewed, revised, and verified the manuscript after using these tools and take full responsibility for its content.

References

1. Khaosod (2021) The Phuket Provincial Agricultural Extension Office is promoting large-scale farming initiatives to boost Phuket pineapples. https://www.khaosod.co.th/pr-news/news_6521603. Accessed 21 July 2021
2. Alloway BJ (2008) Zinc in soils and crop nutrition, 2nd edn. International Zinc Association (IZA), Brussels
3. Sadeghzadeh B (2013) A review of zinc nutrition and plant breeding. J Soil Sci Plant Nutr 13:905–927
4. Australian Pineapples (2006) 10 essential pineapple nutrients. https://www.australianpineapples.com.au/s/10-Essential-pineapple-nutrients.pdf. Accessed 28 May 2025
5. Hafeez B, Khanif YM, Saleem M (2013) Role of zinc in plant nutrition: a review. Am J Exp Agric 3:374–391
6. Guinto DF, Inciong MM (2012) Soil quality, management practices and sustainability of pineapple farms in Cavite, Philippines: Part 1. Soil quality. J South Pac Agric 16:30–41
7. Hassan KM, Gaber SE, Altahan MF, Azzem MA (2020) Single and simultaneous voltammetric sensing of lead(II), cadmium(II) and zinc(II) using a bimetallic Hg-Bi supported on poly(1,2-diaminoanthraquinone)/glassy carbon modified electrode. Sens Bio-Sens Res 29:100345
8. Changshi H, Yiding W, Hongpeng W, Shaojing D, Bo L, Luting Y (2024) Trace Cu^{2+} detection based on GH-PEDOT:PSS-Pt NP-modified glassy carbon electrode. J Mater Sci Mater Electron 35:102
9. Angin YAP, Wijaya K, Trisunaryanti W, Sari RM, Destiarti L, OH WC et al (2025) Enhanced selective Cu(II) detection using a high-performance EDTA/PVA/MWCNT-modified carbon paste electrode. Carbon Lett. https://doi.org/10.1007/s42823-024-00812-z
10. US EPA (2024) Basics of green chemistry. https://www.epa.gov/greenchemistry/basics-green-chemistry. Accessed 26 February 2024
11. Kim S, Jeong Y, Park MO, Jang Y, Bae JS, Hong KS et al (2023) Development of boron doped diamond electrodes material for heavy metal ion sensor with high sensitivity and durability. J Mater Res Technol 23:1375–1385
12. Ai Y, Yan L, Zhang S, Ye X, Xuan Y, He S et al (2023) Ultrasensitive simultaneous electrochemical detection of Zn(II), Cd(II) and Pb(II) based on the bismuth and graphdiyne film modified electrode. Microchem J 184:108156
13. Permwong W, Jakmunee J, Pencharee S (2026) Stripping voltammetric analysis of cadmium on a dual working screen-printed carbon electrode modified with graphene-oxide/carbon-nanohorn composite. Talanta Open 13:100302
14. Tesfaye E, Chandravanshi BS, Negash N, Tessema M (2023) Electrochemical determination of zinc(II) using N_1-hydroxy-N_1,N_2-diphenylbenzamidine and multi-walled carbon nanotubes modified carbon paste electrode. Heliyon 9:e16943

15. Barry SCL, Franke C, Mulaudzi T, Pokpas K, Ajayi RF (2023) Review on surface-modified electrodes for the enhanced electrochemical detection of selective serotonin reuptake inhibitors (SSRIs). Micromachines 14:1416
16. Dueraning A, Kanatharana P, Thavarungkul P, Limbut W (2016) An environmental friendly electrode and extended cathodic potential window for anodic stripping voltammetry of zinc detection. Electrochim Acta 221:133–143
17. Fafa S, Zazoua A (2024) A new electrochemical sensor based on a screen-printed electrode modified with an ion-imprinted PEDOT for the detection and the quantification of Cd(II). Microchem J 204:110996
18. Silva MP, Beluomini MA, Freitas C, Brienzo M, Stradiotto NR (2023) Electrochemical detection of xylobiose in banana biomass using a 3D porous copper oxide foam electrode modified with a molecularly imprinted poly-L-arginine film. J Food Compos Anal 124:105658
19. Doğan HÖ, Ertuğrul B, Çelebi N, Yüksel AK (2025) The electrochemical fabrication of Ag nanoparticles decorated poly(L-cysteine) modified electrode for non-enzymatic H2O2 sensor. Appl Phys A 131:45
20. Zhao H, Jiang Y, Ma Y, Wu Z, Cao Q, He Y et al (2010) Poly(2-amino-4-thiazoleacetic acid)/multiwalled carbon nanotubes modified glassy carbon electrodes for the electrochemical detection of copper(II). Electrochim Acta 55:2518–2521
21. Bounegru AV, Georgescu LP, Iticescu C, Apetrei C (2025) Simultaneous detection of Cu(II) and Pb(II) in the Danube River using a bismuth film modified glassy carbon rotating disk electrode. J Electroanal Chem 979:118873
22. Birara A, Washe AP, Bayeh Y, Ashebr TG (2024) Simultaneous quantification of Cd(II) and Pb(II) by bismuth/poly(bromocresol purple) modified screen-printed carbon electrode in wastewater. Int J Electrochem Sci 19:100412
23. Li Y, Wang Z, Chen X, Yi Z, Wang R (2024) In situ deposition of bismuth on pre-anodized screen-printed electrode for sensitive determination of Cd^{2+} in water and rice with a portable device. Sci Rep 14:18776. https://doi.org/10.1038/s41598-024-69626-7
24. Radovanović MB, Petrović Mihajlović MB, Simonović AT, Tasić Ž, Antonijević MM (2025) Electrochemical detection of cadmium using a bismuth film deposited on a brass electrode. Sensors 25:567. https://doi.org/10.3390/s25010159
25. Eljazouli H, Laabd M, Elamine M, Albourine A (2017) Theoretical approach of the complexation of Zn(II) with a toxic amino acid, l-canavanine and its analogue, l-arginine. J Mater Environ Sci 8:2421–2427
26. US EPA (1996) Method 3050B: Acid digestion of sediments, sludges, and soils. https://www.epa.gov/esam/epa-method-3050b-acid-digestion-sediments-sludges-and-soils. Accessed 10 January 2026
27. Tigari G, Manjunatha JG (2019) Electrochemical preparation of poly(arginine)-modified carbon nanotube paste electrode and its application for the determination of pyridoxine in the presence of riboflavin. J Anal Test 3:331–340. https://doi.org/10.1007/s41664-019-00116-w
28. Khan MZH, Liu X, Tang Y, Zhu J, Hu W, Li X (2018) A glassy carbon electrode modified with a composite consisting of gold nanoparticle, reduced graphene oxide and poly(L-arginine) for simultaneous voltammetric determination of dopamine, serotonin and L-tryptophan. Microchim Acta 185:432. https://doi.org/10.1007/s00604-018-2979-z
29. Kongkaew S, Tubtimtong S, Thavarungkul P, Kanatharana P, Chang KH, Abdullah AFL et al (2022) A fabrication of multichannel graphite electrode using low-cost stencil-printing technique. Sensors 22:8564. https://doi.org/10.3390/s22083034
30. Kongkaew S, Meng L, Limbut W, Liu G, Kanatharana P, Thavarungkul P et al (2023) Craft-and-stick xurographic manufacturing of integrated microfluidic electrochemical sensing platform. Biosensors 13:412. https://doi.org/10.3390/bios13040446
31. Saisahas K, Soleh A, Promsuwan K, Saichanapan J, Phonchai A, Sadiq NSM et al (2022) Nanocoral-like polyaniline-modified graphene-based electrochemical paper-based analytical device for a portable electrochemical sensor for xylazine detection. ACS Omega 7:13913–13924. https://doi.org/10.1021/acsomega.2c00295
32. Saisahas K, Soleh A, Samoson K, Promsuwan K, Saichanapan J, Wangchuk S et al (2025) Sustainable paper-derived laser-induced graphene electrochemical platform for ultra-sensitive diazepam detection in forensic investigations. ACS Omega 10:30944–30957. https://doi.org/10.1021/acsomega.5c03662
33. Dueraning A, Kanatharana P, Thavarungkul P, Limbut W (2014) Bismuth-modified poly(glutamic acid)/glassy carbon electrode for zinc detection by anodic stripping voltammetry. In: International Bioscience Conference (IBSC2014), Phuket, Thailand, pp 397–401
34. Wu KH, Wang JC, Yu SY, Yan BD (2018) A screen-printed carbon electrode modified with a chitosan-based film for in situ heavy metal ions measurement. Int J Environ Agric Biotechnol 3:308–320. https://doi.org/10.22161/ijeab/3.2.1
35. Rahman MA, Won MS, Shim YB (2003) Characterization of an EDTA bonded conducting polymer modified electrode: its application for the simultaneous determination of heavy metal ions. Anal Chem 75:1123–1129. https://doi.org/10.1021/ac0262917
36. Tooley CA, Gasperoni CH, Marnoto S, Halpern JM (2018) Evaluation of metal oxide surface catalysts for the electrochemical activation of amino acids. Sensors 18:3144. https://doi.org/10.3390/s18093144
37. Liu X, Luo L, Ding Y, Ye D (2011) Poly-glutamic acid modified carbon nanotube-doped carbon paste electrode for sensitive detection of L-tryptophan. Bioelectrochemistry 82:38–45. https://doi.org/10.1016/j.bioelechem.2011.05.001
38. Wu Y, Li NB, Luo HQ (2008) Simultaneous measurement of Pb, Cd and Zn using differential pulse anodic stripping voltammetry at a bismuth/poly(p-aminobenzene sulfonic acid) film electrode. Sens Actuators B 133:677–681. https://doi.org/10.1016/j.snb.2008.04.001
39. Guo H, Chen B, Luo Y, Wang R, Tian Q, Chang Y (2024) Effect of Bi(III)-to-metal ion concentration ratios on stripping voltammetric response of bismuth-film glassy carbon electrodes. RSC Adv 14:39361–39371. https://doi.org/10.1039/d4ra07034h
40. Giordano TH, Drummond SE (1991) The potentiometric determination of stability constants for zinc acetate complexes in aqueous solutions to 295 C. Geochim Cosmochim Acta 55:2401–2415. https://doi.org/10.1016/0016-7037(91)90362-9
41. Munoz-Noval A, Fukami K, Kuruma T, Hayakawa S (2024) Structure and complexation mechanism of aqueous Zn(II)-acetate complex studied by XAFS and Raman spectroscopies. Anal Sci 40:1193–1201. https://doi.org/10.1007/s44211-024-00549-z
42. Borrill AJ, Reily NE, Macpherson JV (2019) Addressing the practicalities of anodic stripping voltammetry for heavy metal detection: a tutorial review. Analyst 144:6834–6849. https://doi.org/10.1039/c9an01437c
43. Cao L, Jia J, Wang Z (2008) Sensitive determination of Cd and Pb by differential pulse stripping voltammetry with in situ bismuth-modified zeolite doped carbon paste electrodes. Electrochim Acta 53:2177–2182. https://doi.org/10.1016/j.electacta.2007.09.024
44. Ping J, Wang Y, Wu J, Ying Y, Tu T, Zhang M et al (2014) Development of an electrochemically reduced graphene oxide modified disposable bismuth film electrode and its application for stripping analysis of heavy metals in milk. Food Chem 151:65–71
45. Swartz ME, Krull IS (1997) Analytical method development and validation. CRC, Boca Raton

46. Thanh NM, Hop NV, Luyen ND, Phong NH, Toan TTT (2019) Simultaneous determination of Zn(II), Cd(II), Pb(II), and Cu(II) using differential pulse anodic stripping voltammetry at a bismuth film-modified electrode. Adv Mater Sci Eng 2019:1–11. https://doi.org/10.1155/2019/1826148
47. Seanghirun W, Samoson K, Cotchim S, Kongkaew S, Limbut W (2020) Green electrochemical sensor for Zn(II) ions detection in human seminal fluid. Microchem J 157:104996. https://doi.org/10.1016/j.microc.2020.104958
48. Vanderlaan EL, Nolan JK, Sexton J, Evans-Molina C, Lee H, Voytik-Harbin SL (2023) Development of electrochemical Zn2+sensors for rapid voltammetric detection of glucose-stimulated insulin release from pancreatic β-cells. Biosens Bioelectron 235:115383. https://doi.org/10.1016/j.bios.2023.115409
49. Ringgit G, Siddiquee S, Saallah S, Lal MTM (2022) A sensitive and rapid determination of zinc ion (Zn^{2+}) using electrochemical sensor based on f-MWCNTs/CS/PB/AuE in drinking water. Sci Rep 12:15432. https://doi.org/10.1038/s41598-022-21926-6
50. Vieira D, Allard J, Taylor K, Harvey EJ, Merle G (2022) Zincon-modified CNTs electrochemical tool for salivary and urinary zinc detection. Nanomaterials 12:4456. https://doi.org/10.3390/nano12244431
51. Carhuayal-Alvarez SM, Ascencio-Flores YF, Quiroz-Aguinaga U, Calderon-Zavaleta SL, Muedas-Taipe G, Cardenas-Riojas AA et al (2023) Square-wave voltammetric detection of Zn(II) and Cd(II) with a graphite/carbon paste electrode decorated with 2-hydroxy-1,4-naphthoquinone. ACS ES&T Water 3:2604–2615. https://doi.org/10.1021/acsestwater.3c00140
52. AOAC International (2016) Guidelines for standard method performance requirements. https://www.aoac.org/resources/guidelines-for-standard-method-performance-requirements/. Accessed 15 January 2026
53. US EPA (2018) Method 6010D: Inductively coupled plasma-optical emission spectrometry (ICP-OES), revision 5. U.S. Environmental Protection Agency. https://www.epa.gov/sites/default/files/2018-06/documents/method_6010d_rev_5_0.pdf Washington, DC
54. Huber L (2007) Validation and qualification in analytical laboratories, 2nd edn. Informa Healthcare, New York